Water Soluble Conducting Polymer Nanocomposites: Toward Electronic Understanding for the Catalytic Role of ss-DNA Functionalized Single Walled Carbon Nanotubes

Yufeng Ma, Pui Lam Chiu, Arnaldo Serrano, and Huixin He*
*Chemistry Department, Rutgers University, Newark, NJ 07102
Phone: 973-353-1254; Fax: 973-353-1264
Email: huixinhe@newark.rutgers.edu

ABSTRACT

The intrinsic efficacy of single stranded DNA functionalized single walled carbon nanotubes (ss-DNA/SWNTs) was demonstrated during *in-situ* polymerization of a self-doped polyaniline. Due to the electronic interaction between the monomers, the ss-DNA/SWNTs not only sped up the polymerization, but also significantly improved the quality of the composite. Furthermore, the polymerization in the presence of ss-DNA/SWNTs required less oxidant, indicating that a faster and "greener" polymerization approach can be developed for the production of conducting polymer nanocomposites. These advantages cannot be obtained by post mixing the preformed conducting polymer with ss-DNA/SWNTs. The conductance of the composite prepared from *in-situ* polymerization is almost seven orders of magnitude higher than the mixture prepared from the postmixing approach.

Keywords: carbon nanotubes, DNA, self-doped polyaniline, composite

1 INTRODUCTION

A hot debate aroused recently over the catalytic behavior of carbon nanotubes (CNTs). For a long time people believed that the *electrooxidative* catalytic properties of CNTs can be exploited for a wide variety of applications, including sensors and biosensors. However, recently, Compton and coworkers [1, 2] demonstrated that the origin of the electrocatalytic behavior of CNTs is from the metal catalyst residues, such as iron oxide particles, which remain in the batch after the nanotube fabrication and purification process.

On the other hand, O'Connell and Doorn et al. [3] described the catalytic ability of CNTs in *reduction* of molecules. The catalytic behavior closely related to the electronic structure of CNTs and the ability of oxidized CNTs for oxidation of water. Zheng and his coworkers [4] demonstrated the catalytic property of ss-DNA functionalized SWNTs in photo-induced *reduction* of Ag^+.

Herein, we demonstrated that the single stranded DNA functionalized single walled carbon nanotubes (ss-DNA/SWNTs) acted as *catalytic molecular templates* during polymerization of a self-doped polyaniline. We found that not only was the polymerization rate greatly increased, but also the quality of the resulting polymer was significantly improved. Furthermore, the polymerization in the presence of ss-DNA/SWNTs required less oxidant, ammonium persulfate (APS). These results indicate that a faster and "greener" polymerization approach can be developed for the production of conducting polymer nanocomposites. These advantages cannot be obtained by post mixing the preformed conducting polymer with ss-DNA/SWNTs. We further demonstrated that the efficacy of ss-DNA/SWNTs in the polymerization of a self-doped polyaniline was not due to the catalyst residues (iron oxide particles) present in ss-DNA/SWNTs. It was due to the pre-concentration of monomers along ss-DNA/SWNTs and the electronic interaction between monomers and ss-DNA/SWNTs.

2 EXPERIMENTAL SECTION

2.1 Materials

3-aminophenylbronic acid hemisulfate salt (ABA), potassium fluoride (KF) and all other chemicals were purchased from Aldrich and used as received. Single stranded DNA (ss-DNA) with sequence $d(T)_{30}$ was purchased from Integrated DNA Technologies. All solutions were prepared using deionized water (18.2 MΩ) (Nanopure water, Barnstead).

2.2 Dispersion of SWNTs into water

HiPco Purified single-walled carbon nanotubes (SWNTs) were purchased from Carbon Nanotechnologies and dispersed into water using the method described by Zheng et al, [5] resulting in highly dispersed SWNTs with ss-DNA wrapped. The resulting samples were further dialyzed with a microcon YM-100 centrifugal filter unit (Millipore) to remove free ss-DNA.

2.3 *In-situ* fabrication of a self-doped polyaniline/ss-DNA-SWNTs nanocomposite

A typical synthetic procedure for the preparation of a solution of ss-DNA-SWNTs/PABA nanocomposite is as follows: 50 μL of the solution with ABA (50 mM) and KF (40 mM) in 0.05 M H_2SO_4 was added to 2.5 mL of the ss-DNA/SWNTs solution in 0.05 M H_2SO_4 with a

NSTI-Nanotech 2007, www.nsti.org, ISBN 1420061828 Vol. 1, 2007

concentration of 70 mg/L. The solution was bubbled with nitrogen for 30 min at 0 ºC to remove the dissolved oxygen and mix uniformly. The chemical polymerization of ABA was then initiated by adding 10 µL of 37.5 mM $(NH_4)_2S_2O_8$ (APS) (in 0.05 M H_2SO_4) drop-wise to the mixture. The polymerization was carried out at 0 ºC under nitrogen bubbling for 7 h. Control experiments were also performed to fabricate neat poly (aniline boronic acid) (PABA) under the same conditions without ss-DNA/SWNTs present. The PABA/ss-DNA-SWNT postmixture was prepared by mixing 50 µL of the preformed neat polymer solution with 2.5 mL of the ss-DNA/SWNTs (70 mg/L) in 0.05 M H_2SO_4. The resulting solutions (composite and postmixture) were dialyzed to remove excess salt. 5 µL of the dialyzed solution was placed onto a pre-patterned Si chip (United States Air Force) and dried under vacuum. Then, the conductance of the composite and postmixture were measured with an Electrochemical Workstation CHI 760C.

2.4 *In-situ* monitoring ABA polymerization in the presence/absence of ss-DNA/SWNTs

To study the catalytic effect of ss-DNA/SWNTs, we used a UV-Vis absorption spectroscopy to *in situ* monitor the polymerization processes in the presence/absence of ss-DNA/SWNTs. ABA monomer (2.5 mM or 10 mM) and KF (40mM) were dissolved in 0.5 M H_2SO_4. Then, 91.4 µL of ss-DNA/SWNTs was added to 2.5 mL of the prepared monomer solution. The mixture was bubbled with nitrogen for 30 min and the reaction was initiated by adding 0.5 mL of 37.5 mM APS in 0.5 M H_2SO_4 drop-wise to the mixture. All experiments were performed at 16 ºC. Control experiments were also performed under the same conditions without ss-DNA/SWNTs. All spectra were obtained with a Cary 500 UV-Vis-NIR Spectrophotometer using double beam mode.

3 RESULTS AND DISCUSSION

3.1 Remarkable improved electronic properties of PABA and greatly enhanced rate of polymerization with ss-DNA/SWNTs

The UV-Vis absorption of PABA differs from that of ABA monomers due to the highly conjugated backbone. Therefore, the formation of PABA can be monitored as a function of time with UV-Vis spectroscopy.

Figure 1a shows the *in-situ* UV-Vis spectra recorded at various time intervals for the polymerization of 50 mM ABA in 0.5 M H_2SO_4 (16 °C). During the course of polymerization, the spectra showed two broad bands at 390 nm and 530 nm. The bands increased in intensity with polymerization time. The 530 nm band can be assigned to the excitation of the quinone diimine structure (−N=Q=N−), which is dependent on the overall oxidation state of the polymer. The λ_{max} of the peak at 530 nm was lower compared to the PABA polymerized at 0 °C. This blue shift is consistent with the fact that polymerization at higher temperatures produces polymers with more branched structures, shorter conjugation lengths and higher oxidation states [6]. The absorption peak at 390 nm was assigned to the π-π* excitation of the benzene segment in the formed polymer chains. Interestingly, as time passed, the intensity of this peak is always higher than the peak at 530 nm in the presence of oxidant (APS) and the rate of λ_{max} =390 nm is 3-fold faster than the rate of λ_{max} = 530 nm (Fig. 1a and inset). It is well documented that the formed polymer chains are in the pernigraniline state as long as APS exists in the system. Thus, both peaks should grow at a similar rate in the presence of APS. Therefore, the higher rate at 390 nm compared to that at 530 nm might indicate that another species was also produced during the polymerization. After centrifugation of the polymer solution, a very soluble yellowish product was obtained showing a strong UV absorption peak at 390 nm (Fig. 1d). This peak is characteristic of low molecular weight oligomers existing at high oxidation states. We believe that more oligomers were produced at high temperatures (16 °C, compared to 0 °C). Apparently, the higher rate at 390 nm is due to the overlap of π-π* excitation of benzene segment in the PABA polymers and exiton transition of quinoid segment in the ABA oligomers.

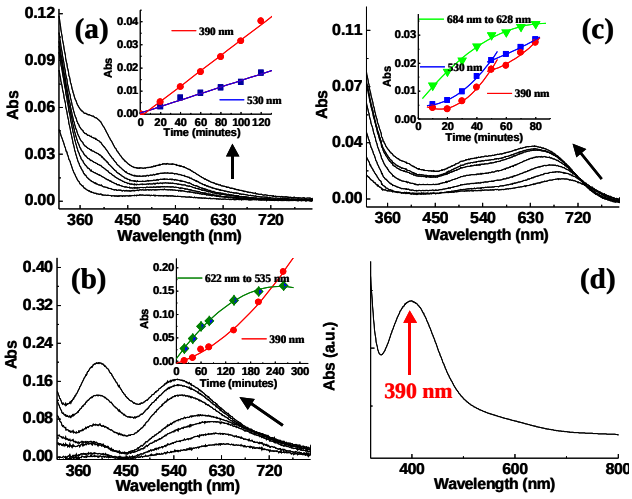

Figure 1: UV-Vis spectroscopy to monitor the polymerization processes at 16 °C, 0.5 M H_2SO_4, (a) 50 mM ABA without SWNTs, (b) the SWNT: ABA weight ratio is 1:200, 10 mM ABA, (c) the SWNT: ABA weight ratio is 1: 50, 2.5 mM ABA. (d) UV-Vis spectrum of the oligomer solution after removing polymer from sample (a).

When the polymerization was performed in the presence of a small amount of ss-DNA/SWNT (SWNT: ABA weight ratio is 1:200, 10 mM ABA), the UV-Vis spectra also showed two broad bands during polymerization (Fig. 1 b). However, the optical absorption spectrum of the polymer changed dramatically upon introduction of nanotubes. The absorption spectrum for the composite is dominated by the

polymer, with little contribution from the nanotubes other than by modifying the absorption of the polymer. Remarkably, the absorption peak of the quinoid exiton transition is greatly red shifted from 530 nm (Fig. 1a) in the neat polymer to 622 nm (bottom spectrum in Fig. 1b) in the composite. One possible explanation for this is that there is a substantial reduction in electron delocalization along the backbone due to the conformational relaxation of the polymer around the nanotube lattice.

The intensity of the peaks remarkably increased with time. The inset in Figure 1b shows the peak intensity as a function of time. Since the absorbance reflects the concentration of PABA formed in the reaction mixture, the slopes of the curves reflect the polymerization rates under different conditions. From this curve we can easily see that the polymerization is 11 times faster with ss-DNA/SWNTs than without ss-DNA/SWNTs, even though the concentration of ABA monomers was 5-fold more diluted. The λ_{max} for the excitation of quinoid units in the polymer was 622 nm at the beginning and gradually shifted to 530 nm, which is the same position as polymerization without ss-DNA/SWNTs. These results may indicate that PABA was first polymerized along nanotubes, thereby having longer conjugation lengths, and existing mainly in the emeraldine state. As time progressed, PABA fully covered the ss-DNA/SWNTs, the influence of ss-DNA/SWNTs on the polymerization diminished, and more "free" PABA was formed. Thus, the blue shifted peak in the 622-535 nm region in Figure 1b resulted from overlapping of excitation of quinoid in "free" polymers (not affected by ss-DNA/SWNTs, 530 nm) and "real" composites (affected by ss-DNA/SWNTs, >530 nm). Once the overlapped peak blue shifted to 530 nm, the peak at 390 nm started to grow faster (Fig. 1b and inset) due to diminution of the influence of ss-DNA/SWNTs, therefore more oligomers produced. By decreasing the monomer concentration to 2.5 mM and increasing ss-DNA-SWNTs/monomer ratio to around 1:50, we can clearly see two different polymer structures (Fig. 1c) simultaneously. The blue shifted peak for "real" composite in the 684-628 nm region showed a similar kinetic curve as in Figure 1b. These remarkable phenomena all supported our assumption described above. Since less oligomer was formed, the absorption peak at 390 nm grew at the same pace as the peak for "real" composite. Interestingly, the peak for "real" composite increased faster than the peak for "free" polymer at 530 nm.

3.2 Ineffective catalytic ability of Fe_2O_3 nanoparticles for polymerization

It was recently reported that the previous claimed electrocatalytic behavior of CNTs might arise from iron oxide impurities rather than from any intrinsic properties of the nanotubes. These impurities were difficult to remove completely. A control experiment was performed with the same concentration of iron oxide as in ss-DNA/SWNTs to verify the catalytic effect of Fe_2O_3 nanoparticles on the polymerization. The results show that the addition of Fe_2O_3 nanoparticles into the solution did not speed up the polymerization rate (data not shown). This indicates that the catalytic effect is not due to the residues, but to the electronic structure of ss-DNA/SWNTs.

3.3 Electronic study of the interaction between ABA monomers and ss-DNA/SWNTs

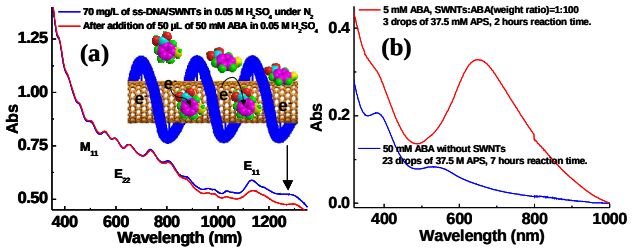

Figure 2: UV-Vis spectra of (a) ss-DNA/SWNTs before (blue) and after (red) addition of ABA monomers under N_2; (b) ABA solutions with (red) and without (blue) ss-DNA/SWNTs after addition of different amount of APS.

To understand the catalytic origin of ss-DNA/SWNTs during the *in-situ* polymerization process, we studied the interaction between ss-DNA/SWNTs and ABA monomers using a UV-Vis-NIR electronic absorption spectroscopy. It has been reported that electron transfer reactions change absorption intensities of CNTs. The UV bleaching sometimes accompanies a red shift of absorption peaks. It is reported that ABA is electron deficient because of the sp^2 hybridization of the boron. Therefore, it is possible that charge transfer complexes would form upon addition of ABA monomers into ss-DNA/SWNT solutions, decreasing the charge density of CNTs and causing the UV-Vis bleaching or the peak position shifting for certain CNTs. The experiment was performed with N_2 bubbling to remove the dissolved O_2 to avoid oxidation of SWNTs. The evolution of the spectrum was monitored upon addition of ABA monomers. Figure 2a shows the UV-Vis-NIR spectra of ss-DNA/SWNT before and after adding ABA monomers under N_2. The peaks at E_{11} and E_{22} are assigned to the first and second van Hove interband transitions of semiconducting (*sem*-) SWNTs, respectively. The peaks at M_{11} (400-600 nm) are assigned to the metallic (*met*-) and semimetallic nanotubes. We found that the *sem*-SWNTs with the first van Hove transitions (1000-1300 nm) experienced bleaching. The absorption intensity was decreased and the peak positions were slightly red shifted after adding ABA (Fig. 2a), and thus the electron density of ABA became higher. However, the electronic properties of *met*-SWNTs remained insensitive to adsorbed ABA monomers. This observation demonstrates that ABA adsorbed along CNTs and the electron transfer occurred from SWNTs to ABA monomers, which are ascribed to the origin of the faster polymerization speed when ss-DNA/SWNTs are present.

NSTI-Nanotech 2007, www.nsti.org, ISBN 1420061828 Vol. 1, 2007

3.4 The role of ss-DNA

It is known that possible interactions of ABA-DNA by a dative bond between NH_2 and boronic acid existed; the interaction could also result in increased electron density of ABA before polymerization. A control experiment was performed with the same concentration of ABA and ss-DNA to study the role of DNA in speeding up the polymerization (data not shown). The results demonstrate that the polymerization speed is similar to that of ABA alone, indicating that the contribution from ss-DNA itself for the increased polymerization rate is very small.

3.5 Less requirement of oxidant by *in-situ* fabrication approach

Notably, less oxidant was needed to form the same amount of polymer when polymerization was performed in the presence of ss-DNA-SWNTs, as shown in Figure 2b. The solution of ABA monomers with ss-DNA/SWNTs was initialized with 3 drops of APS. No further APS was added after initiation. After two hours, the resulting solution was measured by UV spectroscopy (Fig. 2b red). In contrast, APS was added into the pure ABA polymerization for 7 hours (Fig. 2b blue). It is obvious that the polymer yield is much higher with ss-DNA/SWNTs than that without ss-DNA/SWNTs. We believe that this remarkable phenomenon is due to the slower termination process in the chemical polymerization of ABA when ss-DNA/SWNTs are present. The electronic interaction between the monomers and CNTs greatly sped up the generation of radical cations. The pre-alignment of monomers along CNTs also prevented them from collision, which would terminate the polymerization. Furthermore, the electronic interaction between the produced polymer and ss-DNA/SWNTs could stabilize the easily degradable quinoid. These hypotheses are strongly supported by the significantly decreased production of ABA oligomer when polymerized with ss-DNA/SWNTs (Fig. 1c).

3.6 Significant differences in electronic and electrical properties of the composite and the postmixture

To verify whether PABA chains can be attached to the nanotubes by simple physical blending, a control experiment was conducted in which ss-DNA/SWNTs was mixed with the preformed PABA. The UV-Vis-NIR spectra of the composite and postmixture were measured and then the spectrum of ss-DNA/SWNTs at the same concentration was subtracted, resulting with Figure 3a. The PABA in the *in-situ* fabricated nanocomposite is indicative of PABA emeraldine salt adopting a mixture of "compact coil" (820 nm) and "extended coil" conformations (>1000 nm) [7]. The tail (ca 1020 nm) of the band localized in the near IR appeared for the polymer in the *in-situ* fabricated nanocomposite, which has been assigned to delocalized free charge carriers present in secondarily doped PANI. However, the PABA fabricated from postmixing approach only exists in "compact coil" conformation (710 nm) with a higher oxidation state. This result indicates that the nanotemplates can only impose an extended conformation of the polymer chain during polymerization.

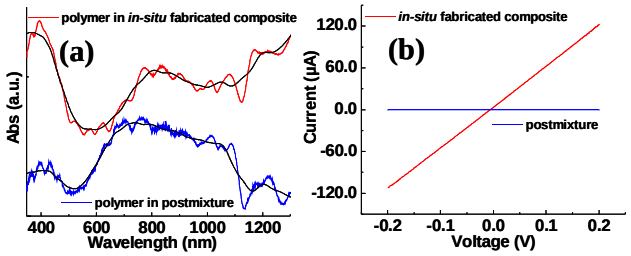

Figure 3: (a) UV-Vis-NIR spectra of PABA in the postmixture and the composite. (b) *I-V* characteristics of the postmixture and the composite films.

Due to the strong interaction with ss-DNA/SWNTs, the PABA in the *in-situ* fabricated composite adopts a more planar conformation, resulting in dramatic enhancement in the conductivity of the composite (Fig. 3b). Figure 3b shows the current-voltage (*I-V*) curves measured on the films prepared from the *in-situ* fabricated composite and postmixture. They all exhibited ohmic behaviors between – 0.2 V and 0.2 V. Remarkably, the electrical conductance of the postmixture film is below 10^{-10} S, and for the composite it is 6.1X 10^{-4} S. The composite from *in-situ* polymerization is almost seven orders of magnitude higher than the postmixture film. The drastic difference in the electrical conductance further indicates that the simple physical blending cannot impart the remarkable electrical properties of CNTs to the mixture.

In summary, this work experimentally demonstrated that the catalytic ability of ss-DNA/SWNTs in the oxidative polymerization of ABA is due to the electronic interaction with ABA monomers, not to the existence of catalytic residues (Fe_2O_3) in ss-DNA/SWNTs. We also demonstrated that the *in-situ* polymerization approach is a faster and greener approach for fabricating genuine composites. The advantages of CNTs cannot be imposed on mixtures by simple postmixing.

REFERENCES

[1] Sljukic, B.; et al., Nano Lett. 6, 1556-1558, 2006.
[2] Banks, C. E.; et al., Angew. Chem. Int. Ed. 45, 2533-2537, 2006.
[3] O'Connell, M.; et al., Nat. Mater. 4, 412-418, 2005.
[4] Zheng, M.; Rostovtsev, V. V., J. Am. Chem. Soc. 128, 7702-7703, 2006.
[5] Zheng, M.; et al., Nat. Mater. 2, 338-342, 2003.
[6] P. N. Adams; et al., Polymer 37, 3411-3417, 1996.
[7] Y. Xia; et al., Chem. Mater. 7, 443, 1995.